Model-based Nonlinear Filter Design for Tower Load Reduction of Wind Power Plants with Active Power Control Capability

Florian Pöschke and Horst Schulte

***Abstract*—In the light of an increasing share in the electrical grid, wind turbines must be enabled to provide grid stabilizing behavior. This can be achieved by a variation of the turbine's power output depending on the current state of the electrical grid. However, changes of power output excite oscillations in the turbine structure. To reduce the loading caused by the considered frequency droop scheme, in this paper a nonlinear model-based filter design in a Takagi-Sugeno structure is proposed. The design uses Lyapunov function-based linear matrix inequalities for deriving the necessary feedback gains of the filter. The results are obtained for NREL's 5 MW reference turbine. By connecting FAST to an analytic power system model, we study the effects on turbine loading as a result of frequency stabilization in case of a load imbalance. The proposed filter is designed and implemented to reduce the damage equivalent load of the tower fore-aft motion, and its influence on the frequency trajectory is studied.**

I. Introduction

The increasing share in the energy generation mix necessitates the provision of ancillary services such as active power control (APC) for grid stabilization from wind turbines [1]. An imbalance of load and generation in the electrical grid results in a frequency deviation, which needs to be coped by appropriate control mechanisms to ensure a stable operation of the electrical power system. While these services are typically designed to act at different timescale, these functionalities involve a variation of the turbine's power output depending on the current state of the electrical grid. Several works have discussed turbines capability to provide APC, e.g., [1]–[6], and provide promising results with regard to the replacement of conventional power plants in the electrical grid. In [1], [3], [4] the authors discuss the possibility to provide frequency control by equipping the wind turbine with a droop control scheme. By adjusting the power output of the turbine based on the current deviation of the grid frequency, the capability of wind turbines to provide frequency stabilization is shown. Despite being valuable contributions for the power system perspective, the wind turbine's mechanical components and the corresponding control interaction is usually portrayed as simple models involving stationary power curves [1]–[5]. Thus, consequences for the loading of the turbine are usually neglected, but are known to be vital for the turbine's lifetime [7], especially if power variation is conducted [6], [8].

F. Pöschke and H. Schulte are with Faculty 1: School of Engineering, Control Engineering Group, University of Applied Sciences Berlin (HTW), D-12459 Berlin, Germany, florian.poeschke@htw-berlin.de, horst.schulte@htw-berlin.de

A variation of the turbine's power output necessarily excites oscillations in the turbine structure. Especially, the strong coupling of the tower fore-aft motion to actuation by pitch [7] represents a cause of additional fatigue loading through frequency stabilizing behavior [8]. To reduce the loading caused by power output feedback to frequency variations, in this contribution a nonlinear model-based filter design in a Takagi-Sugeno structure is discussed. The design uses Lyapunov functions based on linear matrix inequalities for deriving the necessary feedback gains of the nonlinear filter. For this purpose, the filter design is reformulated as feedback control design with respect to a tower model. The deployed linear matrix inequalities enforce a desired damping on the tower motion by design, such that load reduction in operation can be achieved.

The results are obtained for NREL's 5 MW reference turbine [9]. By connecting FAST [10] to an analytic power system model, we study the effects of turbine loading as a result from frequency stabilization in case of a load imbalance. The proposed nonlinear filter is employed to reduce the damage equivalent load of the tower fore-aft motion. Further, the influence of filter on the frequency trajectory is studied.

II. Modeling

A. Takagi-Sugeno Model Framework

Throughout this work, the nonlinear state-space model of the plant, as well as the filter model, are formulated in terms of the Takagi-Sugeno (TS) model structure. TS models provide a useful and uniform framework for nonlinear controller, observer and filter design. Originally introduced in the context of fuzzy systems [11], TS models are weighted combinations of linear submodels and can either be derived from input-output data using system identification techniques [11], [12] or from mathematical models of nonlinear systems. Methods based on linear matrix inequalities (LMIs) stability constraints allow for controller and observer design for TS models [13], [14]. The general TS structure of a state-space model is of the form

$$\dot{x} = \sum_{i=1}^{N} h_i(z) \left(A_i\, x \, + B_i\, u \right) \, , y = \sum_{i=1}^{N} h_i(z)\, C_i\, x \qquad (1)$$

with N linear submodels. Matrices A_i, B_i and C_i of the i-th sub-model have constant coefficients. The vector z of premise variables may comprise states, inputs, and external variables.

978-1-7281-6932-3/20/$31.00 ©2020 IEEE

The functions h_i are the membership functions and fulfill the two conditions [15]

$$\sum_{i=1}^{N} h_i(z) = 1 \,, \tag{2}$$

$$0 \leq h_i(z) \leq 1 \; (i \in \{1, \ldots, N\}) \,, \tag{3}$$

where (2) is the convex sum condition.

In order to obtain the TS structure of a nonlinear model, and provided that a mathematical model is given, there are essentially two ways to derive the linear TS submodels. The first method is local Taylor linearization of the nonlinear model around N stationary points and subsequent fuzzy-blending of the linear submodels to a weighted sum according to (1). Different types of membership functions can be defined, including e.g., triangular, trapezoidal, sigmoid, or Gaussian functions [15]. The second method is the so-called sector nonlinearity approach [16] (and references therein), [17], which yields an exact representation of the nonlinear model.

In this paper we use the first method, whereby the nonlinear model is not explicitly analytically available and therefore the linear models are numerically extracted from the FAST model [10] of the wind turbine.

B. Tower Model

The basis for modeling of the wind turbine tower dynamics in fore-aft direction x_T is provided by N second-order linearized models of the nonlinear system dynamics $\dot{x}_T = f(x_T, \beta, v, \Delta p)$ in the operating points $|_{c_i} := |_{x_{T0i}, \beta_{0i}, v_{0i}, \Delta p_{0i}}$. In a TS description, the dynamics with respect to the pitch angle β, effective wind speed v and power tracking signal Δp is denoted as

$$\begin{aligned} \dot{x}_T = \sum_{i=1}^{N} h_i(z) \big(& \underbrace{\begin{bmatrix} 0 & 1 \\ \frac{\partial f(x_T,\beta,v,\Delta p)}{\partial x_T}|_{c_i} & \frac{\partial f(x_T,\beta,v,\Delta p)}{\partial \dot{x}_T}|_{c_i} \end{bmatrix}}_{A_{Ti}} \\ & \cdot (x_T - x_{T0i}) + \underbrace{\begin{bmatrix} 0 \\ \frac{\partial f(x_T,\beta,v,\Delta p)}{\partial \beta}|_{c_i} \end{bmatrix}}_{B_{Ti}} \cdot (\beta - \beta_{0i}) \big) \end{aligned} \tag{4}$$

where the partial derivatives that specify the dynamics in the i-th operating point are gained by FAST's linearization capability [10].

The system description comprises two premise variables that govern the adjustment to varying dynamics in operation, i.e., $z = [v \;\; \Delta p]^{\mathrm{T}}$. The premise variables span a two dimensional plane, where the investigated number of the operating point on the v-axis and Δp-axis are denoted as i_v and $i_{\Delta p}$ with their maximum number as $i_{v\max} = 54$ and $i_{\Delta p\max} = 15$, respectively. An overview of the considered operating range by a choice of linearization points, and the corresponding pitch angles inducing stationary behavior is given in Fig. 1.

To portray the dependence of the tower motion on a varying power demand Δp that results in a variation of the pitch, the model input is reformulated using κ_i, which is depicted in Fig. 2, as

$$\beta - \beta_{0i} = \kappa_i \Delta p \quad , \tag{5}$$

where the power tracking signal Δp forms the new input to the system description. The operating point dependent gain κ_i is calculated as the mean of the gradients $m_{i_v, i_{\Delta p}}$ depicted in Fig. 2 from power to pitch

$$\kappa_i = \begin{cases} m_{i_v,1} & \text{if } i_{\Delta p} = 1 \\ m_{i_v, i_{\Delta p\max}-1} & \text{if } i_{\Delta p} = i_{\Delta p\max} \\ (m_{i_v, i_{\Delta p}-1} + m_{i_v, i_{\Delta p}})/2 & \text{else} \end{cases} \tag{6}$$

with $i = (1 - i_v) i_{\Delta p\max} + i_{\Delta p}$. As a result, we derive a tower model with the tracking signal Δp as input in form

$$\dot{x}_T = \sum_{i=1}^{N} h_i(z) \big(A_{Ti}(x_T - x_{T0i}) + B_{Ti} \kappa_i \Delta p \big) \quad . \tag{7}$$

C. Grid Model

The power system's frequency is modeled by a dynamic power balance, see e.g., [2]–[4], [6], [18], where a deviation from the electrical synchronous frequency $\Delta\omega = \omega - \omega_s$ can

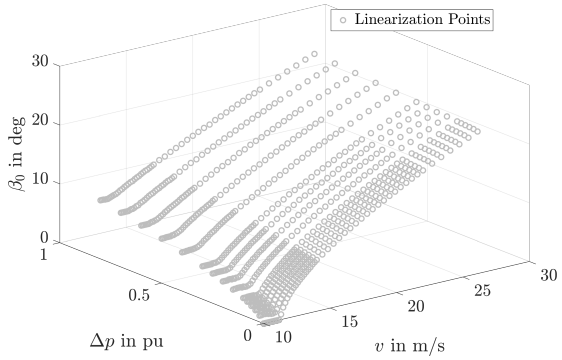

Fig. 1. Linearization points of the wind turbine depending on the wind speed v and power tracking signal Δp. The pitch input values that induce stationary behavior at the given operating points are denoted as β_0.

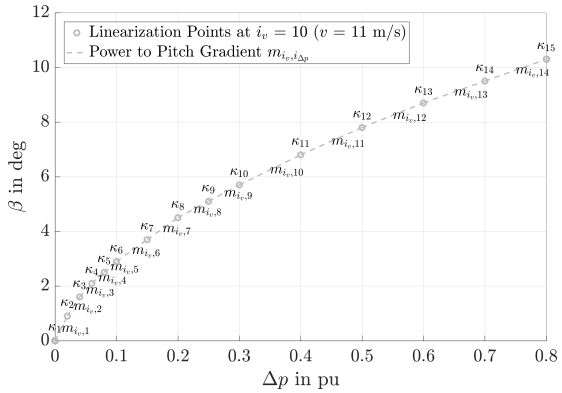

Fig. 2. Linearization points of the wind turbine at a wind speed of 11 m/s. The gain κ_i, which connects a power output variation to a variation in the pitch angle at each operating point, is calculated from the adjacent gradients m_{i-1}, m_i using the stationary pitch angles of the linearization points.

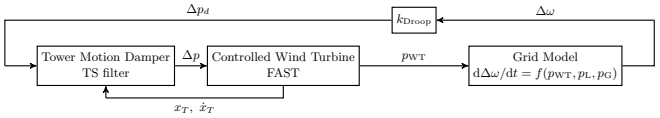

Fig. 3. Overview of the implemented functionality. APC is provided by the wind turbine according to droop k_{Droop} depending on the current frequency deviation of the grid model.

be characterized by the sum of the turbine infeed p_{WT}, power system load p_{L} and power in the grid p_{G}

$$J\frac{\mathrm{d}\Delta\omega}{\mathrm{d}t} = p_{\mathrm{G}} + p_{\mathrm{WT}} + p_{\mathrm{L}} \quad . \tag{8}$$

In that form, the evolution of the grid frequency ω is specified in a normalized description in terms of the inertia J. In accordance with the study in [1], even though we employ simplified dynamics, the excitement of the electrical frequency is initiated by a $\Delta p_{\mathrm{L}} = 10\,\%$ (0.1 pu) load step at a base load of -99.5%. Before the load step, a wind park, represented by one turbine in FAST [10], provides $p_{\mathrm{WT}} = 15\,\%$, while the grid is assumed to provide $p_{\mathrm{G}} = 85\,\%$. The inertia that characterizes the dynamical response of the frequency is chosen to yield a similar dynamical response compared to the initial slope of the frequency in [1] and is found as $J = 10\,\mathrm{s}$.

While in this simplified description of the power system the grid is assumed to provide no stabilizing frequency feedback, i.e., $p_{\mathrm{G}} = \mathrm{const.}$, the wind turbine is equipped with an APC droop control scheme according to the current frequency deviation. This approach emulates an inertial response [3], and thus supports the stabilization of the power grid in case of a frequency event. Depending on the current frequency deviation, the turbine is therefore demanded to vary the current power output by $\Delta p = k_{\mathrm{Droop}}\Delta\omega$, where the proportional gain is defined as $k_{\mathrm{Droop}} = 50$. This corresponds to a power variation of 10% for a frequency deviation of 0.2%, or 0.1 Hz in a 50 Hz-based electrical system. The employed controller for an adjustment of the wind turbine operating point according to Δp varies the generator torque to match the demanded power output, and uses the pitch for balancing of a constant rotational speed in full load region as described in [8]. In that way, the power output can be adjusted to provide APC to the electrical grid. As the filter design is formulated in terms of state feedback, estimated states obtained by a tower observer are used in the scheme. For that purpose, the estimated tower top displacement x_T and speed $\dot{x}_T$ are used in calculation of the filter. An overview of the implemented functionality is given in Fig. 3.

III. Filter Design

The proposed dynamical filter of order n_f is defined as

$$\dot{x}_f = \sum_{i=1}^{N} h_i(z) \underbrace{\begin{bmatrix} 0_{n_f\times 1} & I_{n_f-1} \\ & 0_{1\times n_f-1} \end{bmatrix}}_{A_{fi}} x_f + \underbrace{\begin{bmatrix} 1 \\ \vdots \\ 1 \end{bmatrix}}_{B_{fi}} u \quad , \tag{9}$$

where u is an artificial input, which is subsequently used to shape the dynamical response. The filter employs an integrator chain from the last to the first state of the filter, which is defined as the power tracking signal send to the wind turbine controller, i.e., $\Delta p = x_{f1}$. This allows us to derive a description integrating the nonlinear tower dynamics and filter using (7) and (9) to form

$$\dot{x} = \sum_{i=1}^{N} h_i(z)\Big(\underbrace{\begin{bmatrix} A_{Ti} & B_{Ti}\kappa_i & 0_{n\times n_f-1} \\ 0_{n_f\times n} & & A_{fi} \end{bmatrix}}_{A_i} (x - x_{0i}) + \underbrace{\begin{bmatrix} 0_{n\times 1} \\ B_{fi} \end{bmatrix}}_{B_i} u \Big) \quad . \tag{10}$$

The operating trajectory x_{0i} of $x = [x_T^{\mathrm{T}}\ x_f^{\mathrm{T}}]^{\mathrm{T}}$ is defined by the stationary operating values of the tower derived in the linearization analysis, and the desired filter state. It is adjusted to provide a desired power tracking signal from the APC scheme Δp_d, i.e., $x_{0i} = [x_{T0i}^{\mathrm{T}}\ [\Delta p_d\ 0_{n_f-1\times 1}]^{\mathrm{T}}]$.

System description (10) allows us to formulate the filter design as state feedback controller design employing the input u. For that purpose, a system feedback following the parallel distributed compensation control law [19] is defined

$$u = -\sum_{j=1}^{N} h_j(z) K_j (x - x_{0i}) \quad . \tag{11}$$

Inserting (11) into (10) gives us the closed-loop description of the combined tower and filter dynamics

$$\dot{x} = \sum_{i=1}^{N} h_i(z) \sum_{j=1}^{N} h_j(z)\big((A_i - B_i K_j)(x - x_{0i})\big) \tag{12}$$

under impact of the feedback gains K_j to be synthesized. From a quadratic Lyapunov function candidate $V(x) = x^{\mathrm{T}} X^{-1} x$ with $X = X^{\mathrm{T}} \succ 0$ and the corresponding stability condition $\dot{V}(x) = \dot{x}^{\mathrm{T}} X^{-1} x + x^{\mathrm{T}} X^{-1} \dot{x} \prec 0$ the following LMI stability constraints can be derived [19]

$$X A_i^{\mathrm{T}} + A_i X - M_j^{\mathrm{T}} B_i^{\mathrm{T}} - B_i M_j \prec 0 \quad , \tag{13}$$

where X and M_j are variables to be found. If a solution is obtained by one of various available LMI solvers [20], the necessary feedback gains are calculated from $K_j = M_j X^{-1}$ and stability is verified. Additional LMIs can be used to enforce a desired dynamical response of the closed-loop system. For that purpose, the maximum decay rate of the system can be restricted to $\alpha_{\max}$ by

$$X A_i^{\mathrm{T}} + A_i X - M_j^{\mathrm{T}} B_i^{\mathrm{T}} - B_i M_j \succ -2\alpha_{\max} X \quad , \tag{14}$$

which is conducted to ensure a proper operation within the numerical environment that the filter is applied. Further, a desired damping on the closed-loop system in operation actively

provided by the controller can be formulated in terms of LMIs as [21]

$$\begin{bmatrix} \sin\theta(\Gamma_1) & \cos\theta(\Gamma_2) \\ \cos\theta(\Gamma_2^{\mathrm{T}}) & \sin\theta(\Gamma_1) \end{bmatrix} \prec 0 \tag{15}$$

with

$$\begin{aligned} \Gamma_1 &= \left(A_i X - B_i M_j + X A_i^{\mathrm{T}} - M_j^{\mathrm{T}} B_i^{\mathrm{T}}\right) \\ \Gamma_2 &= \left(A_i X - B_i M_j - X A_i^{\mathrm{T}} + M_j^{\mathrm{T}} B_i^{\mathrm{T}}\right) \end{aligned} .$$

The desired damping D is formulated in terms of the angle Θ, that can be calculated according to $\Theta = \arccos(D)$ [21]. It is used to provide damping to the tower dynamics by purposefully shaping the combined tower and filter dynamics through the feedback.

The filter design parameters used for the system (12) are a desired damping of at least $D = 12\%$, a maximum decay rate of $\alpha_{\max} = 100$ for the LMIs (13), (14) and (15). The filter is designed of second order, i.e., $n_f = 2$. The LMI solver yields N feedback gains K_j along with the characterization of the Lyapunov function

$$X = \begin{bmatrix} 1.8675 & -0.602 & -0.3815 & -1.1197 \\ -0.602 & 7.7337 & 6.4277 & 5.0647 \\ -0.3815 & 6.4277 & 8.8484 & 3.2063 \\ -1.1197 & 5.0647 & 3.2063 & 14.9906 \end{bmatrix} \succ 0 \quad .$$

IV. Results

A. Constant Inflow

Fig. 4 depicts the system response to a load imbalance in the electrical grid at a constant wind of 18 m/s. Due to a lack of stabilizing mechanisms without APC, i.e., continuing nominal power production of the wind turbine, the frequency grows continuously at a slope defined by the inertia J in (8). The application of APC by the wind turbine is capable of arresting the frequency at 50.7 Hz with the employed slope k_{Droop}. The involved reduction to 30% of the power production can be observed in Fig. 4 (d). As one turbine is modeled to provide $p_{\mathrm{WT}} = 15\,\%$ before the load step, the stationary output after the disturbance in the electrical grid corresponds to a total power of $p_{\mathrm{WT}} = 4.5\,\%$. In combination with the power provided by the electrical grid $p_{\mathrm{G}} = 85\,\%$, this yields the demanded power of the load $p_{\mathrm{L}} = 89.5\,\%$. While the APC scheme without applying the filter arrests the frequency at 50.69 Hz, the filtering and thus the differing evolution of the power tracking signal results in a frequency of 50.7 Hz.

Frequency stabilization, however, is conducted at the cost of exciting the structural dynamics of the turbine. As the motion of the tower top in fore-aft direction displays in Fig. 4 (e), without the proposed filter the tower top shows a lightly damped oscillation while converging to the altered operating point. The application of the proposed filter, on the other hand, results in an increase of damping, and consequently a smoother transition into the new operating point.

This simulation study in constant wind was repeated for inflow with 14 m/s, 16 m/s and 20 m/s. The resulting damage equivalent loads in the considered scenarios are depicted in Fig. 5. The load analysis reveals a significant decrease along the considered operating range in tower fore-aft loading through the implementation of the proposed filter. The reduction capabilities by applying the filter in constant wind speeds are in a range of 10.5% at 20 m/s and 13% at 16 m/s.

B. Turbulent Inflow

By exciting the turbine with turbulent inflow in identical grid scenarios, the impact of grid stabilization and resulting loads in usual operating conditions of wind turbines can be studied. The varying wind speed, depicted in Fig. 6 (a), excites the structural dynamics of the turbine. In addition to a reaction on the frequency deviation, the tower top deflection in fore-aft direction in Fig.6 (e) is caused by an interference of the two effects. Despite an additional fluctuation due to the turbulent inflow and thus power production, the frequency evolution in combination with the power produced by the turbine after the load step in the grid is in line with the results obtained at constant wind speed.

In Fig. 7 the deviation of the power tracking signal due to the applied filter can be observed. As the evolution of the tower fore-aft motion is used in the filter (see Fig. 3), an actuation for providing tower damping is also observed before the load imbalance occurs at t=50 s. While the initial slope of the power tracking signal is very similar compared to applying the scheme without filtering, an excitation of the tower motion due to the variation of the operating point causes a deviation of the two signals, which effectively results in a reduction of the loading experienced by the turbine tower.

To identify the additional loading through APC in turbulent wind conditions, the resulting damages are normalized to the loads *without* a variation of the power output due to a frequency deviation in Fig. 8 (b). An increase of up to 70% at a wind speed of 14 m/s can be observed. As previously reported for the scenarios in constant wind, the TS filter reduces the damage equivalent loads significantly, e.g., 40% reduction at 14 m/s compared to APC without filter. Especially where additional loading due to APC is most striking in lower wind speeds, the model-based filter is capable of mitigating the effects of frequency stabilization. This decreases for medium wind speeds where the additional loading due to APC is small, indicating the stochastic nature of the wind as main source of loading in this operational range. As stated for the state evolution in turbulent inflow, the damage results from an interaction of the grid, turbine and wind dynamics.

V. Discussion

The presented results reveal the additional fatigue loading due to application of the droop control scheme in stabilization of the electrical frequency. Especially in lower wind speed, where the pitch magnitudes (see Fig. 1) and the distance traveled by the tower due to the changing operating points are greatest, this causes severe additional fatigue loading. It is, however, interesting to notice that ultimate loading of the tower was not negatively affected in the considered scenarios. Except for a slight increase of 1.7% at turbulent inflow with a

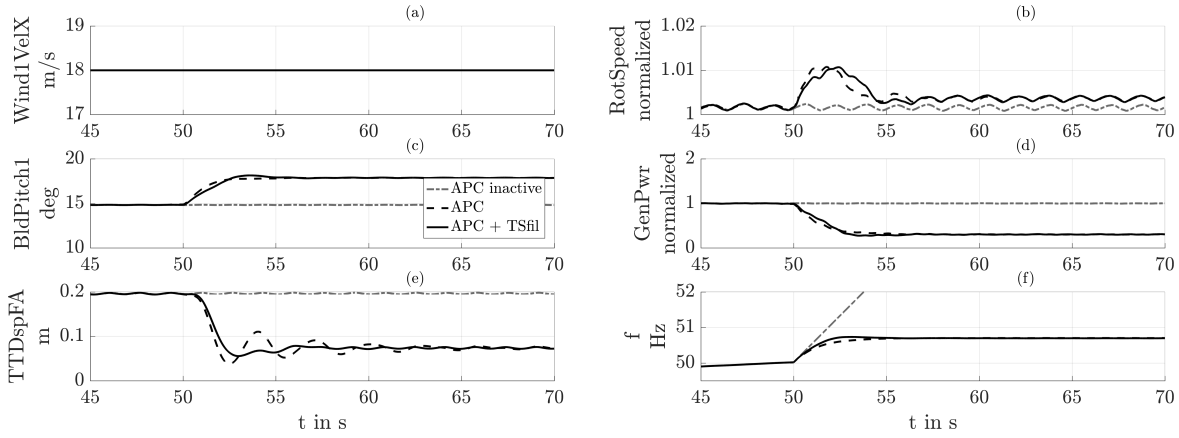

Fig. 4. Response to a power system load imbalance at t = 50 s and constant wind excitement at 18 m/s. Subplots: (a) downwind hub-height wind speed (b) normalized rotational speed (c) blade 1 pitch angle (d) normalized power output (e) tower-top fore-aft deflection (f) frequency of the grid model

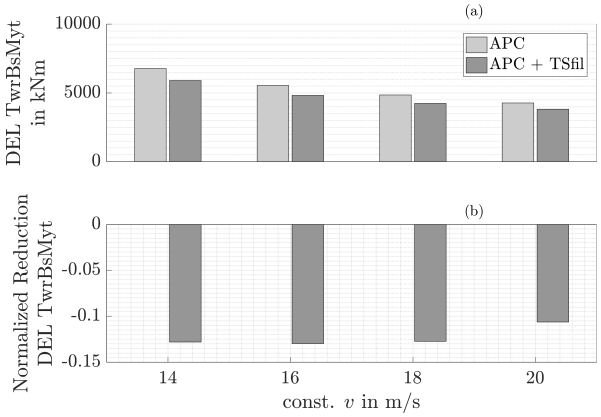

Fig. 5. Comparison of the tower base fore-aft moment DELs at different constant wind speeds with a power system load imbalance as depicted in Fig. 4. Subplots: (a) DEL tower base fore-aft moment (b) reduction of DEL normalized to APC operation without applying filter.

mean of 21 m/s, ultimate tower loading in fore-aft direction was identified to decrease, ranging up to 24% at a mean turbulent wind of 18 m/s.

In case of constant wind, the damping characteristics of the designed filter shows similar fatigue load reduction along the considered operating range. In turbulent inflow conditions, however, the fatigue loading and the reduction yield are less distinct. As noticed, the loads are caused by an interference of the turbulent wind excitement and the power output demand of the APC scheme, where especially in medium wind the excitement from the wind overshadows the effects from frequency stabilization.

The proposed model-based concept integrates the varying dynamics in the filter design, and thus directly accounts for the characteristics of the considered system in the design step. While the focus in this contribution is on the tower oscillation in fore-aft direction, the basic filter design can be enhanced to include more dynamical effects of the wind turbine, e.g., drivetrain oscillation. By calculation of the membership functions in operation of the TS scheme, a natural approach for handling the varying system dynamics is given and consequently, the need for separate scheduler design or tuning of operating point dependent filter loops is avoided.

By reformulation of the filter design as state feedback control scheme, commonly applied LMIs can be used in the filter design. The basic stability constraints restrict the filter dynamics to the left half of the complex plane. While this ensures stability, the range of accessible closed-loop dynamics is indefinite, leaving great design freedom to the LMI solver. For that reason, the application of LMIs that enforce a desired dynamical behavior of the closed-loop system is central to the proposed concept. Especially the LMIs imposing an active damping to the control scheme provide an effective constraint design possibility with regard to load reduction capabilities from the considered scheme.

VI. Conclusion

In this contribution, the effects of grid stabilizing behavior are studied from a mechanical loading perspective of wind turbines. By equipping the turbine with a droop control scheme, the power output of the turbine is varied according to the current state of the electrical grid frequency. The results show that this feedback enables the turbine to arrest the frequency in a simple analytical grid model. While the output power variation excites the structural dynamics of the turbine, a model-based nonlinear filter in a TS structure is proposed to reduce the resulting loading.

For that purpose, a tower model is reformulated to include the variable power demand as an input to the system. Subsequently, the combined tower and filter dynamics are described, and a feedback control design employing LMIs is used as filter design procedure. This allows for the application of commonly used LMIs for feedback design to the filter design problem.

While the APC functionality increases the fatigue loading of the tower especially in fore-aft direction, the simulation results underline the capability of the proposed filter to reduce the damage by enforcing an active damping from processing the demanded power tracking signal in the filter before passing it to the wind turbine controller.

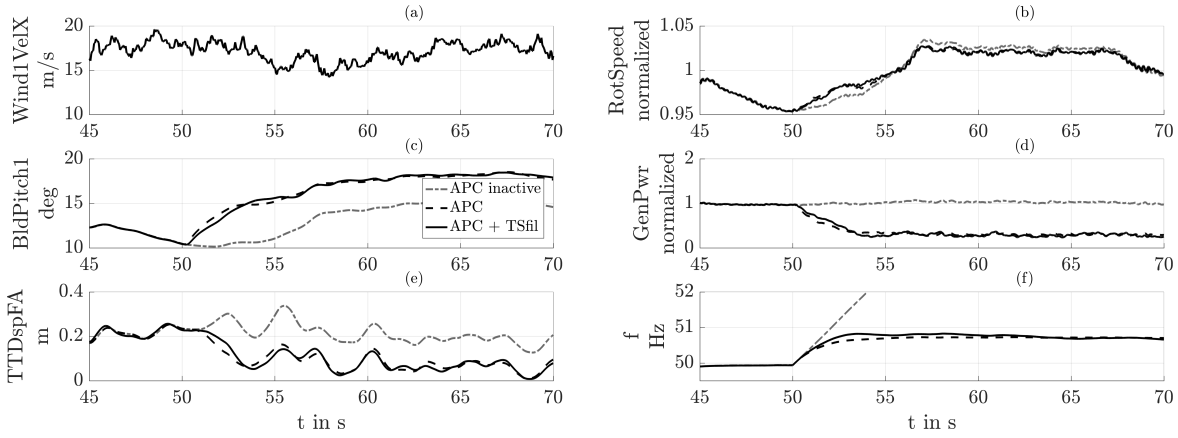

Fig. 6. Response to a power system load imbalance at t = 50 s and turbulent wind with a mean of 18 m/s. Subplots: (a) downwind hub-height wind speed (b) normalized rotational speed (c) blade 1 pitch angle (d) normalized power output (e) tower-top fore-aft deflection (f) frequency of the grid model

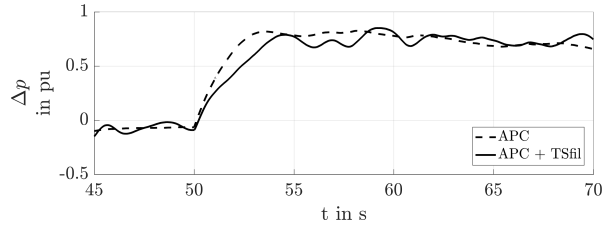

Fig. 7. Comparison of the power tracking signal Δp processed by the controller with and without application of the filter.

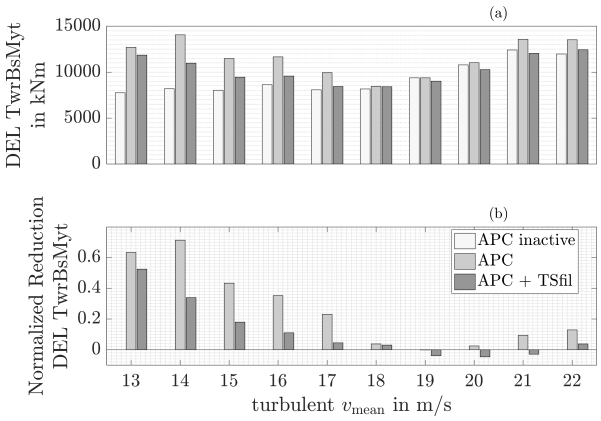

Fig. 8. Comparison of the tower base fore-aft moment DELs at different turbulent wind speeds with a power system load imbalance, see Fig. 6.

REFERENCES

[1] J. Morren, J. Pierik, and S. de Haan, "Inertial response of variable speed wind turbines," *Electric Power Systems Research*, vol. 76, no. 11, pp. 980 – 987, 2006.

[2] P. Keung, P. Li, H. Banakar, and B. T. Ooi, "Kinetic energy of wind-turbine generators for system frequency support," *IEEE Transactions on Power Systems*, vol. 24, no. 1, pp. 279–287, Feb 2009.

[3] J. Van de Vyver, J. D. M. De Kooning, B. Meersman, L. Vandevelde, and T. L. Vandoorn, "Droop control as an alternative inertial response strategy for the synthetic inertia on wind turbines," *IEEE Transactions on Power Systems*, vol. 31, no. 2, pp. 1129–1138, March 2016.

[4] P. Li, W. Hu, R. Hu, Q. Huang, J. Yao, and Z. Chen, "Strategy for wind power plant contribution to frequency control under variable wind speed," *Renewable Energy*, vol. 130, pp. 1226 – 1236, 2019.

[5] H. Luo, Z. Hu, H. Zhang, and H. Chen, "Coordinated active power control strategy for deloaded wind turbines to improve regulation performance in agc," *IEEE Transactions on Power Systems*, vol. 34, no. 1, pp. 98–108, Jan 2019.

[6] X. Wang, Y. Wang, and Y. Liu, "Dynamic load frequency control for high-penetration wind power considering wind turbine fatigue load," *International Journal of Electrical Power & Energy Systems*, vol. 117, p. 105696, 2020.

[7] E. A. Bossanyi, "Wind turbine control for load reduction," *Wind Energy*, vol. 6, no. 3, pp. 229–244, 2003.

[8] F. Pöschke, E. Gauterin, M. Kühn, J. Fortmann, and H. Schulte, "Load Mitigation and Power Tracking Capability forWind Turbines using LMI-based Control Design," *Wind Energy*, 2020, to be published.

[9] J. M. Jonkman, S. Butterfield, W. Musial, and G. Scott, "Definition of a 5-MW Reference Wind Turbine for Offshore System Development," National Renewable Energy Laboratory, Tech. Rep., 2009.

[10] J. M. Jonkman and M. L. Buhl, "FAST Users Guide," National Renewable Energy Laboratory, Tech. Rep., 2005, https://nwtc.nrel.gov/system/files/FAST.pdf (9 September 2019).

[11] T. Takagi and M. Sugeno, "Fuzzy Identification of Systems and Its Application to Modeling and Control," *IEEE Transactions on Systems, Man, and Cybernetics*, vol. 15, no. 1, pp. 116–132, 1985.

[12] M. Sugeno and G. T. Kang, "Structure identification of fuzzy models," *Fuzzy Sets and Systems*, vol. 28, pp. 15–33, 1988.

[13] H. O. Wang, K. Tanaka, and M. F. Griffin, "An Approach to Fuzzy Control of Nonlinear Systems: Stability and Design Issues," *IEEE Transactions on Fuzzy Systems*, vol. 4, no. 1, pp. 14–23, 1996.

[14] K. Tanaka, T. Ikeda, and H. Wang, "Fuzzy regulators and fuzzy observers: Relaxed stability conditions and lmi-based design," *IEEE Transactions on Fuzzy Systems*, vol. 6, pp. 250–265, 1998.

[15] Z. Lendek, T. M. Guerra, R. Babuška, and B. De Schutter, *Stability Analysis and Nonlinear Observer Design Using Takagi-Sugeno Fuzzy Models*. Springer-Verlag Berlin Heidelberg, 2010.

[16] K. Tanaka and M. Sano, "A Robust Stabilization Problem of Fuzzy Control Systems and Its Application to Backing up Control of a Truck-Trailer," *IEEE Transactions on Fuzzy Systems*, vol. 2, no. 2, pp. 119–134, 1994.

[17] K. Tanaka and H. O. Wang, *Fuzzy Control Systems Design and Analysis: A Linear Matrix Inequality Approach*. John Wiley & Sons, Inc, 2001.

[18] J. Machowski, J. Bialek, and J. Bumby, *Power System Dynamics: Stability and Control*. John Wiley & Sons, Ltd, 2008.

[19] K. Tanaka and H. O. Wang, *Fuzzy Control Systems Design and Analysis: A Linear Matrix Inequality Approach*. John Wiley & Sons, Inc., 2001.

[20] J. G. VanAntwerp and R. D. Braatz, "A tutorial on linear and bilinear matrix inequalities," *Journal of Process Control*, vol. 10, no. 4, pp. 363 – 385, 2000.

[21] M. Chilali and P. Gahinet, "H_∞ design with pole placement constraints: an LMI approach," *IEEE Transactions on Automatic Control*, vol. 41, no. 3, pp. 358–367, Mar 1996.